The importance of the film structure during self-powered Ibuprofen salicylate drug release from polypyrrole electrodeposited on AZ31 Mg

B Alshammary[1], N. Casillas[2], R.B. Cook[3], J. Swingler[4], C. Ponce de León[1], F.C. Walsh[1, 3]

[1] *Energy Technology Research Group, Engineering Sciences, Faculty of Engineering and the Environment, University of Southampton, Highfield, Southampton SO17 1BJ, UK.*

[2] *Departamento de Quimica, Universidad de Guadalajara*
Centro Universitario de Ciencias Exactas e Ingenierias (CUCEI)
Blvd. Marcelino Garcia Barragan #1451
Guadalajara, Jalisco, Mexico, CP. 44430.

[3] *National Centre for Advanced Tribology at Southampton (nCATS)and Materials Engineering Research Group, Faculty of engineering and the Environment, University of Southampton, Highfield, Southampton SO17 1BJ, UK.*

[4] *School of Engineering and Physical Sciences, Herriot-Watt University*
Edinburgh, EH14 4AS, UK

ABSTRACT

Therapeutic drugs uploaded into conjugated conductive polymer matrices deposited on active magnesium alloys serve as controlled dose, self-powered drug delivery systems. Preferentially drugs are added into polymer films in the largest amount possible, mostly to prevent long-term treatments. However, added drugs might interact with the polymer matrix affecting either the structure or the final mechanical properties of the polymer film. In this work polypyrrole films (PPy) electrodeposited on an AZ31 Mg alloy in ibuprofen and salicylate containing solutions are investigated in terms of their uploading capacity, surface morphology and mechanical properties. The techniques used to investigate the uploaded PPy films include cyclic voltammetry (CV), SEM, EDS and depth-sensing indentation (DSI). A maximum ibuprofen concentration of 440±40 μg cm^{-2} was obtained in PPy films in the presence of sodium salicylate. The release fraction of ibuprofen as a function of time is fitted to Avrami's equation. The hardness and reduced modulus decreased by 54% and 40% respectively, when the Ppy films are prepared in the presence of sodium ibuprofen compared with those prepared in sodium salicylate only, indicating a more plastic film with ibuprofen.

Key words: conductive polymer, corrosion, drug release, electrodeposition, ibuprofen, magnesium alloy, polypyrrole, self-powered, salicylate.

1. Introduction

Polymer films electrodeposited on active metal alloys and uploaded with various ionic therapeutic drugs are the subject of current investigations [1-3]. Some of them are encouraged by the development of biodegradable, biodisposable self-powered drug-delivery systems [1]. The operation mechanism of self-powered systems relies on a galvanic coupling between conductive polymers films deposited on the surface of an active alloy. Therapeutic drugs are uploaded as dopants into the film, while the polymer is growing by attracting counterions to balance the charge [4-6]. Once a self-powered system is implanted in a corrosive environment, as the one encountered inside the human body, or on the surface of the skin, it undergoes corrosion. The corroding active alloy pumps electrons to reduce the polymer, contracts and releases the therapeutic drug. Accordingly, a sufficient corrosion resistance alloy act as a biodegradable implant and in combination with a polymer film serve as vehicle to deliver drugs such as risperidone, dexamethasone, pain relievers or antibiotics [1,4].

Typical alloys for self-powered drug release include, Mg (97% Mg, 2% Al, 1% Zn) [1], Mg (99.9% purity) [2], sputtered Mg thin films [5] and AZ91D and AZ31 Mg alloys [7,8]. These alloys are attractive as they match the mechanical properties of the human bones. For instance, Mg alloys and the human bone have an approximate density of 1.74-2.00 g cm^{-3} and 1.8-2.1 g cm^{-3} respectively, and an elastic modulus of 41-45 GPa and 130-180 GPa, respectively. Moreover the compressive yield strength of Mg is 65-100 GPa while the human bones is 3-20 GPa [9]. One concern however, is the corrosion of biodegradable Mg alloys that can release undesirable metals such as Al, so biocompatible alloys having a low Al content, such as AZ31 Mg alloy, are desirable for biomedical applications [10,11].

Polypyrrole is one of the most common, biocompatible and mechanically robust conductive polymers (CPs) which has been used for corrosion protection of metals [12,13,7,14] and local drug delivery [4]. The size, steric effects, functional groups, charge and chemical structure of the uploaded drug may affect the polymer nucleation and growth processes and its mechanical properties [13]. The depth-sensing indentation (DSI) technique can be used to determine the mean hardness (H) and reduced modulus (E_r) of PPy films electrodeposited under different circumstances [15-17].

During the electrodeposition of the conductive polymer film on active magnesium alloys, two competitive processes occur; the nucleation and growth processes of the polymer and the dissolution of the metal. Dopant ions such as salicylate and oxalate form a passive layer on the Mg surface and allow the polymerisation [18,19]. However, when drugs are present in solution, they might be absorbed on the surface of the active magnesium alloys affecting the CPs electrodeposition [20]. It has been reported in the literature that ibuprofen affects the polymerisation and structure of poly(3,4-ethylenedioxythiophene) (PEDOT) and poly(3,4-ethylenedioxypyrrole) PEDOP matrices [6,21]. Thus, the amount of drug incorporated into CPs needs to be optimized [22]. Several alternatives have been suggested to increase the amount of the drug on the polymer such as nanostructure CPs [22] or addition of cationic surfactants [23] or heparin that increases the cation exchange capacity [24].

The aim of this paper is to investigate the effects of sodium ibuprofen in the morphological structure, mass fraction release rate and mechanical properties of electrodeposited PPy films on AZ31 Mg alloys in 0.5 mol dm^{-3} sodium salicylate solution at different IBU

concentrations, 0.5-50 x10^{-6} mol dm^{-3}. The novelty of this paper is to highlight the effects of ibuprofen on the quality and properties of PPy films deposited on AZ31-Mg alloy.

2. Experimental

Pyrrole monomer (Sigma Aldrich) was double-distilled and stored in a dark flask at low temperature, under a nitrogen atmosphere. Sodium ibuprofen, (Fluka), sodium salicylate (Aldrich) and acetone (Fisher Scientific) were analytical grade and used as received. All solutions were prepared with 18 mΩ cm (O Purite) deionized water. A 250 μm thick AZ31 Mg alloy foil (Goodfellow) substrate was used in all experiments.

A three-electrode glass electrochemical cell connected to a potentiostat/galvanostat PGSTAT30 (EcoChemie, Netherlands) was used. The working electrode was the AZ31 Mg alloy while a 1 cm^2 platinum mesh was the counter electrode and a saturated calomel electrode (SCE) the reference. Prior to the electrochemical experiments, the AZ31 Mg alloy foil was wet polished with a series of SiC sand paper down to 2000 grade and degreased with acetone, rinsed with deionized water and sonicated for 10 minutes. The samples were tape masked to expose a constant area of 1 cm^2 and positioned vertically within 2 cm distance from the platinum mesh counter electrode. The polymerization solution consisted of a mixture of 0.5 mol dm^{-3} pyrrole (Py), 0.5 mol dm^{-3} sodium salicylate (SA) and sodium ibuprofen (IBU) at concentrations of 0.5, 1, 10 and 50 × 10^{-3} mol dm^{-3} (hereafter named as: SA, SA-Py and SA-Py-xIBU, where x is the millimolar concentration). A rest time of 600 s was routinely applied to all the samples prior to each electrochemical experiment. The PPy films were grown potentiodynamically with a continuous N_2 stream bubbling in solution to remove dissolved O_2 that may affect the oxidation rate of Py or the AZ31 Mg alloy. The

linear potential sweep started at -0.5 V towards +1.0 V *vs.* SCE at a scan rate of 20 mV s^{-1} for 20 cycles until the film reached a thickness of *ca.* 20±5 μm, as determined by SEM and optical imaging. All measurements were made at room temperature (295 K).

Scanning electron micrographs were obtained with a JEOL JSM-6500F FEG-SEM instrument equipped with an EDS x-ray analyser, operating under a vacuum of <0.12 Pa and an accelerating voltage of 5 keV. A nanoTest Vantage system (Micro Materials Ltd., Wrexham, UK) was used to characterize the mechanical properties of the PPy films. The indentations were performed in load control mode using a 5 μm radius spherical tip to a maximum load of 3×10^{-3} N, at a loading rate of 0.12×10^{-3} N s^{-1}, with a 100 s holding time at maximum load. A total of 20 indents were performed on each sample, the results reported correspond to the mean value with a standard deviation.

The ibuprofen (IBU) contained in the PPy films prepared on 1 cm^2 of the AZ31 Mg alloy was released in 20 cm^3 of 0.9 wt. % NaCl. Several aliquots of 5 cm^3 were collected at regular intervals of time and in order to keep the same volume and the sample completely immersed in solution, the volume was replenished by an equal amount of fresh NaCl solution. The samples were analysed in a Neosys-2000, UV-VISIBLE Spectrophotometer, Scinco Co. Ltd. The concentrations of IBU and SA were determined spectrophotometrically at wavelengths of 222 and 295 nm, respectively, using calibration curves. Since SA shows absorption at 222 nm wavelength, it was necessary to subtract its absorbance at this wavelength in order to determine the IBU concentration. The reported data correspond to an average of at least three experiments. The PPy films were characterised by with a Nicolet 360 FTIR

spectrophotometer and the spectra compared with spectra reported elsewhere in the literature [7,8].

3. Results and discussion

3.1 Electrochemical characterisation

Open-circuit potential (OCP) measurements of the AZ31 Mg alloy in SA-Py, and SA-Py xIBU solutions obtained during the 600 s rest period are illustrated in Fig. 1. Although AZ31 Mg alloys are naturally active in aqueous media and possess extremely high negative redox potentials, the presence of species capable of forming a stable protective layer, contributes to the displacement of the OCPs to nobler values [8,18,19]. The AZ31 Mg alloy in SA-Py solution displays an OCP of -1.75±0.022 V *vs.* SCE which rapidly changes to a less negative value of -1.619±0.002 V *vs.* SCE as is seen in curve (a) of Fig. 1. A similar trend can be observed for an AZ31 Mg alloy immersed in SA-Py-(0.5–50)IBU solutions (Fig. 1b)-f)). The OCP for solutions with IBU content of 0.5 and 1.0×10^{-3} mol dm^{-3} (curves b and c), is similar to that in SA solutions (curve a), but for concentrations above 10×10^{-3} mol dm^{-3} IBU, the OCP becomes much more noble reaching -1.26 V *vs.* SCE after 600 s as shown in Fig. 1f) for 50×10^{-3} mol dm^{-3} IBU. This occurs because passive hydroxide/oxide and salicylate magnesium chelate films, which can further diminish the magnesium dissolution, contribute to the equilibrium at the alloy/solution interface [18,19]. No oscillations, indicating breakdown and reconstruction of the passive layer, were seen during the OCP measurements. The increase of the OCP with increasing concentration suggests that the IBU contributes to the passivation of the magnesium surface. Before growing a stable compact PPy film on the

surface of an AZ31 Mg alloy, it is critical to leave the sample at the OCP for at least 600 s in the SA solution to passivate the surface, otherwise an incomplete PPy film will be formed.

Cyclic voltammograms (CVs) of an AZ31 Mg alloy in three different electrolytes are shown in Fig. 2. In an SA solution, curve (a), a large oxidation peak at *ca.* -0.35 V *vs.* SCE due to the oxidation of a non-passivated Mg alloy, which is far away from the OCP (-1.62 V *vs.* SCE) can be seen. Mg ions react with salicylate in solution forming a low solubility chelate complex that precipitates on the metal surface [18]. At +0.8 V *vs.* SCE an extended second anodic process is due to the oxidation of salicylate ions in solution [8]. This process is irreversible because there is no reduction peak. The analysis of the oxidation peak at -0.35 V *vs.* SCE at different potential sweep rates shows that the peak does not follow a linear relationship with the scan rate nor with the square root of the scan rate in the range of 10-70 mV s^{-1}. This suggest that the oxidation is neither a diffusion-controlled process nor an adsorption, instead, it confirms that the formation of the passivating chelate layer on the alloy limits diffusion of magnesium ions and forms a stable magnesium chelate complex. The peak shifts towards less negative potentials as the scan rate increases, which is consistent with an irreversible process [25].

The CVs responses for solutions containing SA-Py (curve b) and SA-Py-0.5IBU (curve c) in Figure 2 exhibit a similar broad oxidation peak at slightly positive potentials, *ca.* -0.3 V *vs.* SCE and lower current density compared to the SA solution (curve a) due to formation of the salicylate complex. In these solutions, nucleation and growth of the PPy film at a potential at *ca.* +0.8 V *vs.* SCE takes place [8,25]. The nucleation and growth processes are evidenced by the crossing potentials at +0.8 V and +0.73 V *vs.* SCE for SA-Py and SA-Py-0.5IBU

solutions respectively, during the reverse scan towards negative values [8]. At more positive values than the PPy nucleation and crossing potentials, there is a rapid increase in the current due to the polymerisation of Py and the dissolution of the underlying AZ31 Mg alloy. The two solutions seem to follow a similar trend, but a higher current density was observed for SA-Py and a more blunt reversal current wave for SA-Py-0.5IBU, indicating that less PPy film was formed on the electrode in the presence of IBU.

3.2 Influence of concentrations IBU

Figs. 3a and 3b show a series of CVs acquired in solutions with higher IBU concentrations, i.e., 10 and 50 × 10^{-3} mol dm^{-3}, respectively. The first cycles for both concentrations do not present the characteristic peak due to the formation of the Mg salicylate film and the current density, due to the polymerisation of PPy is very low specially during the first cycles, at more than +0.8 V *vs*. SCE, as seen in Fig. 2. This suggests that IBU not only affects the formation of the passive salicylate adsorbed layer, but also the nucleation and growth of the PPy film. As the number of cycles increases the solution with 10 × 10^{-3} mol dm^{-3} IBU shows a slight increase in current density due to the polymerisation of Py at > +0.8 V *vs*. SCE. However, the PPy film does not form a uniform coating on the AZ31 Mg alloy surface. Instead, a series of randomly distributed black PPy spots with poor adherence and several cracks were formed, which readily detached from the surface revealing underlying corrosion products. Figure 3b shows that an increase in the IBU concentration up to 50 × 10^{-3} mol dm^{-3} the formation of the PPy film is completely inhibited. Similar results have been reported in the literature on the effect of IBU on the electropolymerisation of PEDOP-IBU films, where the polymerization is suppressed at high IBU concentrations and films with lower charge

capacity are formed [21]. This effect has been explained in terms of a transition between the ibuprofen acting as a dopant and becoming a non-dopant inclusion [21]. In this case, the salicylate layer was absent and the current density was substantially reduced without any potential crossings that denote the PPy nucleation and growth. It can be speculated that IBU is adsorbed in the Mg alloy limiting the access of Py to the electrode surface. In addition, the incorporation of IBU into the polymer structure, either as a dopant or inclusion, also limits the growth processes of the polymer likely due to steric effects. IBU is a large molecule in comparison with other counter ions, such as Cl^- or ClO_4^- used to balance the charge during the polymerisation and changes nucleation and growth processes [26,27,21].

SEM micrographs of PPy films prepared in SA-Py and SA-Py-0.5IBU solutions are shown in Fig. 4a)-d). The PPy films formed from SA-Py solutions are black, compact, crack-free and adherent, see Fig. 4a). High magnification SEM micrographs of these films, see Fig. 4b), reveal a globular surface morphology characteristic for PPy films [8]. On the contrary PPy films formed in solutions containing ibuprofen shows uneven surfaces with some scattered pits and cracks as shown in the SEM micrograph in Fig. 4c). Higher magnification SEM images of this films displayed a mixture of cylindrical, needle-like structures with sizes in the order of 3 μm length and 0.5 μm diameter randomly distributed on the surface. These images show the effect of low concentrations of ibuprofen on the film structure which confirms the influence of IBU on the nucleation and growth of PPy films. It can be suggested that IBU induces a change of nucleation of Py from a 2-dimensional, in which the surface is covered by globular cauliflower shape structure to a 3-dimensional nucleation forming cylindrical needle-like structures. Similar polymerisation effects were reported by Chebil *et*

al. using perchlorate and bisphosphate as dopant ions on Ni [26]. The average film thickness reached for the samples after 20 cycles was *ca*. 20±5 μm for the films formed in SA-Py and SA-Py-0.5IBU solutions measured by SEM and optical microscope for cross sectioned samples. Analogous conjugated polymer systems, such as PEDOP-IBU, develop a roughening of the surface after releasing the IBU either from the surface or the bulk polymer [21].

3.3 Drug uploading and release

SA and IBU are uploaded into the PPy film during polymerisation to balance the charge of the polymer backbone. Fig. 5 shows a horizontal bar plot illustrating the experimental results of the liberation of the IBU when the PPy film was synthetized in the presence of different concentrations of IBU. The left hand side shows the concentrations of IBU (i.e., 0.0, 0.5, 1.0 and 5.0×10^{-3} mol dm^{-3}) used in solution to prepare the films in the presence of SA-Py. On the right hand side, the figure shows the total amount of IBU released in 0.9 wt. % NaCl solution after 200 hours. The calculated amount of PPy deposited potentiodynamically on 1 cm^2 area of the AZ31 Mg alloy was 3.0×10^{-3} g. The highest load is 414×10^{-6} g/cm^2 of IBU for sample 4 which correspond to a ratio of 138×10^{-3} g g^{-1} (IBU/PPy). This value is within the range of concentration of dopants in PPy films which varies from a few $\times 10^{-9}$ g to several $\times 10^{-3}$ g, either for nanostructured or chemically assisted drug uploading in PPy films [1,23]. On the other hand, IBU released after 5 min elapsed-time from a 1 cm^2 drug-loaded matrix from PEDOP-IBU system is between 21.8 ±1.3 to 25±1.3 x10^{-6} g $cm^{-2,}$ more than one order of magnitude smaller than in this work, for PPy-IBU-SS films [21]. These large differences are likely due to a more substantial inclusion of IBU in the film besides the charge storage capacity and expected differences between the release efficiency of both films. Other

examples of the amount of drug than can be uploaded on PPy films include neurotrophin-3 with a value of 25×10^{-9} g cm^{-2} on gold coated Mylar at a PPy film of 3.6–26 $\times 10^{-6}$ m thickness [22]. Another one is methotrexate on PPy films with a loading capacity of 24.5 $\times 10^{-3}$ g g^{-1} [23] and chlorpromazine with 191±7 $\times 10^{-3}$ g on a 0.126 cm^2 Pt disc coated with 8±2 $\times 10^{-6}$ m thick PPy film [24].

IBU was released from 20±5 x10^{-6} m PPy film deposited on one side of 1 cm^2 AZ31 Mg alloy immersed in a 0.9% NaCl solution. The other side of the alloy was bared and exposed to the NaCl solution. Fig. 6 shows a release profile curve of mass fraction of drug released as a function of time. At short periods of time (<50 minutes), the rate of release is high and tends to level off. This result is consistent with previous reports in the literature denoting a rapid release at the initial stages for dexamethasone in 10% wt. NaCl solutions and other systems [1,4,28]. Self-powered systems rely on the dissolution of the substrate metal to reduce the polymer film and release the incorporated drug. Any through porosity or cracks in the PPy film can also provide a pathway for chloride ions to diffuse through to the substrate metal and promote crevice and pitting corrosion in the PPy/AZ31 Mg alloy interface [28,29]. This increases the corroding area above the fixed area at the back of the sample. Moreover, it also accounts for a large scattering in the data for the release fraction at larger periods of time, where the error bars enlarge substantially likely due to the unpredictable corrosion rate (see Fig. 6 for t >250 min). This is consistent with previous results reported in the literature which shows large scattering at longer times, for self-powered systems [1].

Avrami's equation (1) was used as a model to represent the fraction release profile *X* for samples prepared using a concentration of 0.5×10^{-3} mol dm^{-3} IBU. This equation was initially proposed to analyse and predict crystallization processes, but it can also fit well to diffusion controlled and potential-assisted drug release data, particularly for PPy in salicylate media and different types of drugs [30,31,24]. Both Avrami's parameter, *n,* and the release constant, *k,* are obtained from the slope and intercept of the Avrami's plot of ln[-ln(1-*X*)] *vs.* ln *t*.

$$X = 1 - exp(-kt^n) \quad (1)$$

According to the literature, for diffuse controlled drug release systems, the Avrami's parameter, *n,* varies from 0.54 to 1 (first order), depending on the contribution of the diffusion [30,31,24]. In the case of self-powered release, the constant, *k,* is equal to 0.125, which is within the reported values for potential-assisted release processes of ionic drugs, but the Avrami parameter, *n,* kinetic order parameter, is equal to 0.11, much smaller than values reported in the literature [31,24]. Besides these differences, Avrami's equation describes the trend of the experimental data obtained for the self-powered IBU release from PPy films. The contribution of potential difference and diffusion in self-powered release systems can be expected due to potential variations across the film [4].

3.4 Depth-sensing indentation (DSI)

The mechanical properties of the PPy films are dependent on the chemical structure, molecular size and dopant ion concentration [17], [15]. To investigate the effect of ibuprofen

in the PPy film, a series of 20 indentations along randomly selected sampling lines were performed on IBU-free and IBU loaded PPy films. Fig. 7 shows load-displacement curves obtained from PPy films uploaded with different amounts of ibuprofen. For each sample the 3×10^{-3} N load resulted in a different depth of penetration, with the maximum depth of the indents in the 5×10^{-3} mol dm^{-3} doped sample being less than 1μm, the indentation interaction volume being confined to the PPy film and not influenced by the substrate.

Table 1 summarizes the average hardness (H), reduced modulus (E_r) and the ratio between H and E_r of the films investigated, as well as the concentration of IBU in solution and contained in the PPy film. Comparison of the mechanical properties of ibuprofen-free PPy films with those containing large amounts of ibuprofen (414×10^{-6} g), showed a decrease in the H and E_r ratio of 54% and 40%, respectively. The (H/E_r) increases 66% denoting a softer more elastic material. Theoretically, the addition of ibuprofen into the PPy film increases the free space in the polymer matrix and modifies the structure of the PPy film [15,17] sodium ibuprofen is a large molecule with a single charge, when added into the PPy matrix acts as an additional ion dopant along with the sodium salicylate ions to balance the polymer charge. The size of the ibuprofen molecule however results in an increase in the gap between the polymer chains, reducing the strength of the attractive forces between them making polymer chain motion and deformation easier than IBU-free polymer films [15,17]. As previously shown *vide supra*, in the absence of ibuprofen, PPy films in SA media developed a uniform, compact, adherent, globular-like structure (Fig. 4a)-b)). In contrast, the addition of ibuprofen into the PPy film produces a less compact, less adherent, cylindrical, needle-like structure in Fig. 4c)-d). There are few reports in the literature concerning the role that dopant ions play in PPy in terms of their effects on molecular conformations, charge location and structural

defects in the polymer chain [32,33]. Usually, ion dopants induce changes in the polymer conformation that result in either a better alignment or increased misalignment of the polymer chains and contribute to additional packaging or unpacking of the polymer matrix [32]. The mechanical properties of the PPy films can be also modified by the electrosynthesis method used to prepare the film or by additional heat treatments [34]. This provides the opportunity to prepare films which are optimized in terms of their elasticity for specific purposes, such as a more corrosion protective films or more reliable drug delivery systems.

4. Conclusions

The effects of sodium ibuprofen on the quality of the electrodeposited PPy films were characterised. A high loading IBU capacity in the PPy films is desirable for long-term therapeutical treatments. The amount of IBU incorporated into the PPy film in this work is higher than that reported in the literature for other drugs or IBU loaded in PEDOP and PEDOT matrices. However, additions of IBU to the solution affect the electrodeposition processes of the film. A transition from a globular to cylindrical morphology in a PPy film has been observed for IBU concentrations in solution $>1 \times 10^{-3}$ mol dm^{-3}. Larger IBU concentrations of 50×10^{-3} mol dm^{-3} completely inhibit formation of the PPy film. Avrami's equation provides an appropriate fit to the experimental IBU fraction released from a PPy film in 0.9 wt. % NaCl solutions. IBU also produces substantial changes in the mechanical properties of the PPy film compared with IBU-free PPy films. The results indicate up to 54% reduction in H, 40% reduction in Er, and an increase of 66% of H/Er. An increment of the polymer free volume is the major cause for diminishing the mechanical properties of the PPy film. The outcomes from this investigation require the modelling of a self-powered drug

release mechanism and theoretical predictions of the effects of uploaded drugs on polymer matrix structure using density functional theory and mechanical models in order to provide a more thorough understanding of the system.

5. Acknowledgments

The authors gratefully acknowledge the financial support provided by the Ministry of Higher Education and the Ministry of Health of Saudi Arabia. Support for a sabbatical leave for NCS from the National Council of Science and Technology of Mexico (CONACyT) and Exportadora de Postes S.A. de C.V. are greatly appreciated.

References

1. Moulton SE, Imisides MD, Shepherd RL, Wallace GG (2008) Galvanic coupling conducting polymers to biodegradable Mg initiates autonomously powered drug release. Journal of Materials Chemistry 18 (30):3608-3613. doi:10.1039/B805481A

2. Luo X, Cui XT (2011) Electrochemical deposition of conducting polymer coatings on magnesium surfaces in ionic liquid. Acta Biomaterialia 7 (1):441-446.

3. Tian P, Liu X (2015) Surface modification of biodegradable magnesium and its alloys for biomedical applications. Regenerative Biomaterials 2 (2):135-151

4. Asplund M, Boehler C, Stieglitz T (2014) Anti-inflammatory polymer electrodes for glial scar treatment: bringing the conceptual idea to future results. Frontiers in neuroengineering 7

5. Svirskis D, Travas-Sejdic J, Rodgers A, Garg S (2010) Electrochemically controlled drug delivery based on intrinsically conducting polymers. Journal of Controlled Release 146 (1):6-15.

6. Krukiewicz K, Zak JK (2014) Conjugated polymers as robust carriers for controlled delivery of anti-inflammatory drugs. Journal of Materials Science 49 (16):5738-5745.

7. Turhan MC, Weiser M, Killian MS, Leitner B, Virtanen S (2011) Electrochemical polymerization and characterization of polypyrrole on Mg–Al alloy (AZ91D). Synthetic Metals 161 (3–4):360-364.

8. Srinivasan A, Ranjani P, Rajendran N (2013) Electrochemical polymerization of pyrrole over AZ31 Mg alloy for biomedical applications. Electrochimica Acta 88:310-321.

9. Staiger MP, Pietak AM, Huadmai J, Dias G (2006) Magnesium and its alloys as orthopedic biomaterials: A review. Biomaterials 27 (9):1728-1734.

10. Bondy SC (2016) Review: Low levels of aluminum can lead to behavioral and morphological changes associated with Alzheimer's disease and age-related neurodegeneration. Neurotoxicology 52:222-229.

11. Grogan JA, O'Brien BJ, Leen SB, McHugh PE (2011) A corrosion model for bioabsorbable metallic stents. Acta Biomaterialia 7 (9):3523-3533.

12. Jiang Y, Guo X, Wei Y, Zhai C, Ding W (2003) Corrosion protection of polypyrrole electrodeposited on AZ91 magnesium alloys in alkaline solutions. Synthetic Metals 139 (2):335-339

13. Herrasti P, Kulak AN, Bavykin DV, Ponce de Léon C, Zekonyte J, Walsh FC (2011) Electrodeposition of polypyrrole–titanate nanotube composites coatings and their corrosion resistance. Electrochimica Acta 56 (3):1323-1328.

14. Alshammary B, Walsh FC, Herrasti P, Ponce de Leon C (2015) Electrodeposited conductive polymers for controlled drug release: polypyrrole. Journal of Solid State Electrochemistry:1-21

15. Uzun O, Başman N, Alkan C, Kölemen U, Yılmaz F (2011) Investigation of mechanical and creep properties of polypyrrole by depth-sensing indentation. Polymer bulletin 66 (5):649-660

16. Yang S, Zhang Y-W, Zeng K (2004) Analysis of nanoindentation creep for polymeric materials. Journal of applied physics 95 (7):3655-3666

17. Gandhi M, Spinks G, Burford R, Wallace G (1995) Film substructure and mechanical properties of electrochemically prepared polypyrrole. Polymer 36 (25):4761-4765

18. Cascalheira AC, Abrantes LM (2004) The electrochemical behaviour of copper in sodium salicylate aqueous solutions. Electrochimica Acta 49 (27):5023-5028.

19. Gao H, Li Q, Chen F, Dai Y, Luo F, Li L (2011) Study of the corrosion inhibition effect of sodium silicate on AZ91D magnesium alloy. Corrosion Science 53 (4):1401-1407

20. Bui TX, Choi H (2010) Influence of ionic strength, anions, cations, and natural organic matter on the adsorption of pharmaceuticals to silica. Chemosphere 80 (7):681-686

21. Krukiewicz K, Zawisza P, Herman AP, Turczyn R, Boncel S, Zak JK (2016) An electrically controlled drug delivery system based on conducting poly (3, 4-ethylenedioxypyrrole) matrix. Bioelectrochemistry 108:13-20

22. Thompson BC, Moulton SE, Ding J, Richardson R, Cameron A, O'Leary S, Wallace GG, Clark GM (2006) Optimising the incorporation and release of a neurotrophic factor using conducting polypyrrole. Journal of Controlled Release 116 (3):285-294.

23. Alizadeh N, Shamaeli E (2014) Electrochemically controlled release of anticancer drug methotrexate using nanostructured polypyrrole modified with cetylpyridinium: Release kinetics investigation. Electrochimica Acta 130:488-496. doi:10.1016/j.electacta.2014.03.055

24. Shamaeli E, Alizadeh N (2014) Nanostructured biocompatible thermal/electrical stimuli-responsive biopolymer-doped polypyrrole for controlled release of chlorpromazine: Kinetics studies. International journal of pharmaceutics 472 (1):327-338

25. Bard AJ, Faulkner LR (2001) Electrochemical methods: fundamentals and applications. Department of Chemistry and Biochemistry University of Texas at Austin, John Wiley & Sons, Inc:156-176

26. Chebil S, Monod M, Fisicaro P (2014) Direct electrochemical synthesis and characterization of polypyrrole nano-and micro-snails. Electrochimica Acta 123:527-534

27. Licona-Sánchez TdJ, Álvarez-Romero G, Mendoza-Huizar L, Galán-Vidal C, Palomar-Pardavé M, Romero-Romo M, Herrera-Hernández H, Uruchurtu J, Juárez-García J (2010) Nucleation and growth kinetics of electrodeposited sulfate-doped polypyrrole: determination of the diffusion coefficient of SO42− in the polymeric membrane. The Journal of Physical Chemistry B 114 (30):9737-9743

28. Singh I, Singh M, Das S (2015) A comparative corrosion behavior of Mg, AZ31 and AZ91 alloys in 3.5% NaCl solution. Journal of Magnesium and Alloys 3 (2):142-148

29. Ding Y, Wen C, Hodgson P, Li Y (2014) Effects of alloying elements on the corrosion behavior and biocompatibility of biodegradable magnesium alloys: a review. Journal of Materials Chemistry B 2 (14):1912-1933

30. Lorenzo AT, Arnal ML, Albuerne J, Müller AJ (2007) DSC isothermal polymer crystallization kinetics measurements and the use of the Avrami equation to fit the data: Guidelines to avoid common problems. Polymer testing 26 (2):222-231

31. Shamaeli E, Alizadeh N (2013) Kinetic studies of electrochemically controlled release of salicylate from nanostructure conducting molecularly imprinted polymer. Electrochimica Acta 114:409-415

32. Colle R, Curioni A (1998) Density-functional theory study of electronic and structural properties of doped polypyrroles. Journal of the American Chemical Society 120 (19):4832-4839

33. Smith JR, Li Y, Cox PA, Campbell SA, Breakspear S, Whitley DC, Walsh FC (2011) Electrochemical and computational studies of electrically conducting polymer coatings. Transactions of the Institute of Metal Finishing 89 (5):244-248.

34. Herrasti P, Dıaz L, Ocón P, Ibáñez A, Fatas E (2004) Electrochemical and mechanical properties of polypyrrole coatings on steel. Electrochimica acta 49 (22):3693-3699

Table 1 Mechanical properties of PPy films.

Concentration, $\times 10^{-3}$ **mol dm^{-3}**	**Ibuprofen,** 10^{-6} **g**	**Hardness (*H*), GPa**	**Reduced modulus (E_r), GPa**	***H*/E_r ratio**
0	0	0.37 ± 0.09	10.2 ± 1.72	0.03
0.5	254 ± 20	0.29 ± 0.07	9.4 ± 2.14	0.03
1	260 ± 20	0.32 ± 0.04	7.8 ± 0.76	0.04
5	414 ± 40	0.20 ± 0.02	4.1 ± 0.36	0.05

Figure captions

Figure 1 OCP *vs.* time for an AZ31 Mg alloy in 0.5 mol dm^{-3} Py, 0.5 mol dm^{-3} SA with different sodium xIBU concentrations a) 0, b) 0.5, c) 1, d) 5, e) 10 and f) 50×10^{-3} mol dm^{-3} monitored over 10 minutes.

Figure 2 First cycle voltammogram of an AZ31 Mg alloy in: a) 0.5 mol dm^{-3} SA, b) 0.5 mol dm^{-3} SA and 0.5 mol dm^{-3} Py, c) 0.5 mol dm^{-3} SA, 0.5 mol dm^{-3} Py and 0.5×10^{-3} mol dm^{-3} IBU at a potential sweep rate of 20 mV s^{-1}.

Figure 3 Cyclic voltammetry for an AZ31 Mg alloy for 20 cycles at a potential sweep rate of 20 mV s^{-1} in a solution containing 0.5 mol dm^{-3} SA, 0.5 mol dm^{-3} Py with a) 10×10^{-3} mol dm^{-3} IBU and b) 50×10^{-3} mol dm^{-3} IBU. The electrode was immersed in the solution for 10 minutes before starting.

Figure 4 SEM micrographs of the surface of the PPy film formed electrochemically on an AZ31 Mg alloy in 0.5 mol dm^{-3} SA and 0.5 mol dm^{-3} Py (a)-(b) and 0.5 mol dm^{-3} SA, 0.5 mol dm^{-3} Py and 0.5×10^{-3} mol dm^{-3} IBU (c)-(d) by cyclic voltammetry in a potential range of −0.5 to 1 V *vs.* SCE at a potential sweep rate of 20 mV s^{-1} for 20 cycles.

Figure 5 Left hand side identification number *vs.* concentration used to prepare the PPy film and right hand side total amount of IBU released for the film for period of 200 hrs in 0.9% wt. NaCl solution.

Figure 6 Mass fraction of IBU released from a 1 cm^2, ≈ 20 x10^{-6}m thick PPy film grown in 0.5 mol dm^{-3} SA, 0.5 mol dm^{-3} Py and 0.5 × 10^{-3} mol dm^{-3} IBU. Drug delivery was performed in a 0.9% wt. NaCl solution at 296 K. Experimental results represent the mean values and a standard deviations over at least 3 replicas.

Figure 7 Load-displacement curves for PPy films prepared at different IBU concentrations: a) 0, b) 0.5, c) 1.0 and d) 5 × 10^{-3} mol dm^{-3} at a constant load of 3 × 10^{-3} N.

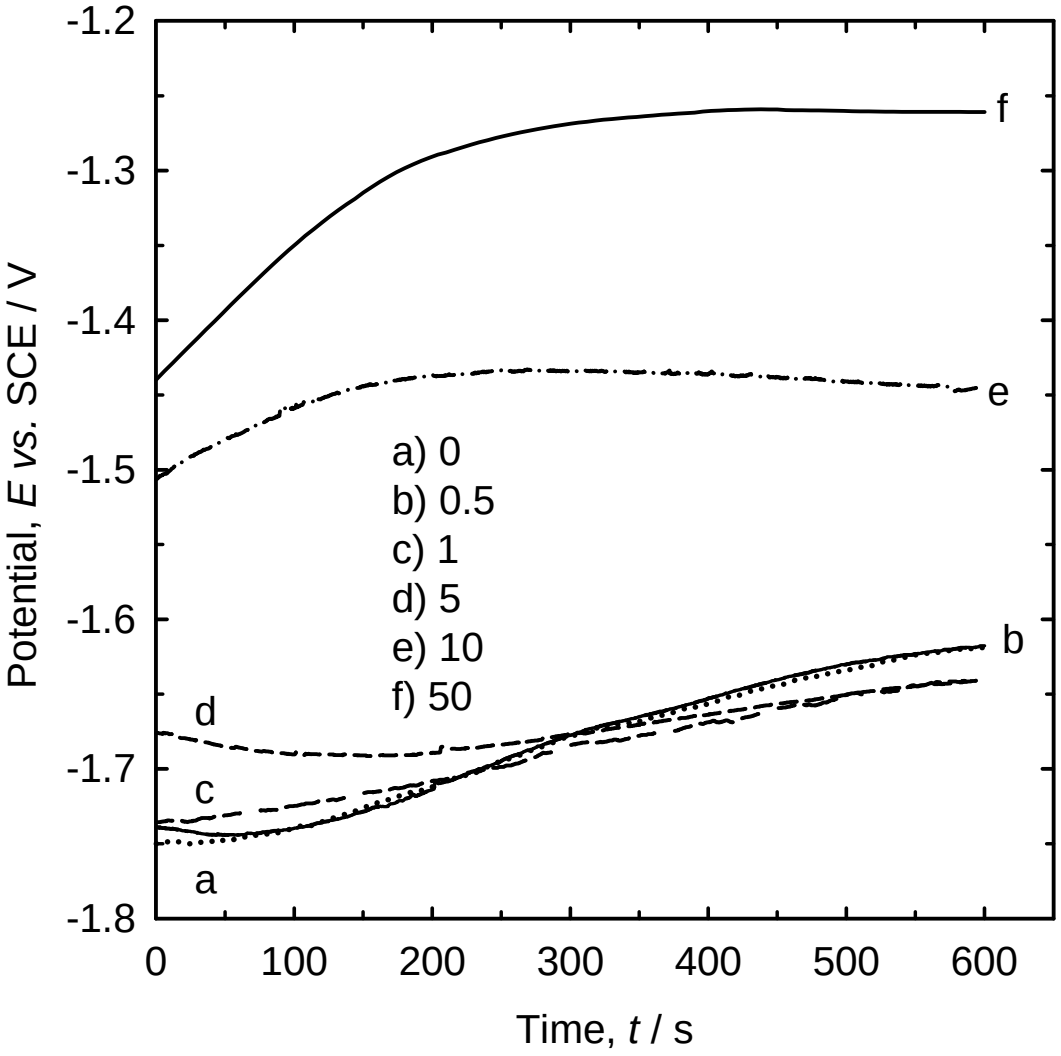
-1.2
-1.3
-1.4
-1.5
-1.6
-1.7
-1.8
Potential, E vs. SCE / V
0
100
200
300
400
500
600
Time, t / s
a) 0
b) 0.5
c) 1
d) 5
e) 10
f) 50
a
b
c
d
e
f

Figure 1

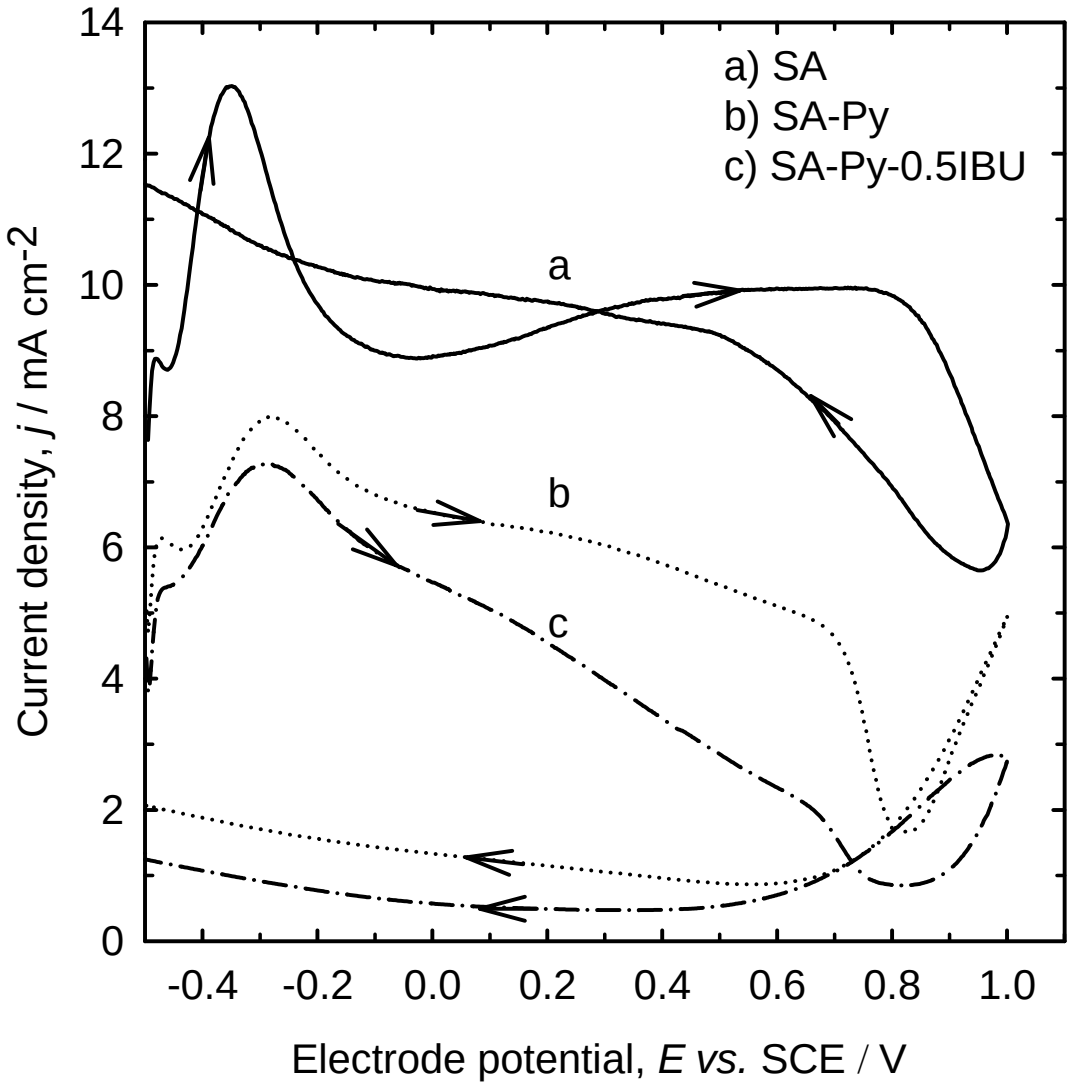
a) SA
b) SA-Py
c) SA-Py-0.5IBU
a
b
c
Current density, j / mA cm-2
Electrode potential, E vs. SCE / V
0
2
4
6
8
10
12
14
-0.4
-0.2
0.0
0.2
0.4
0.6
0.8
1.0

Figure 2

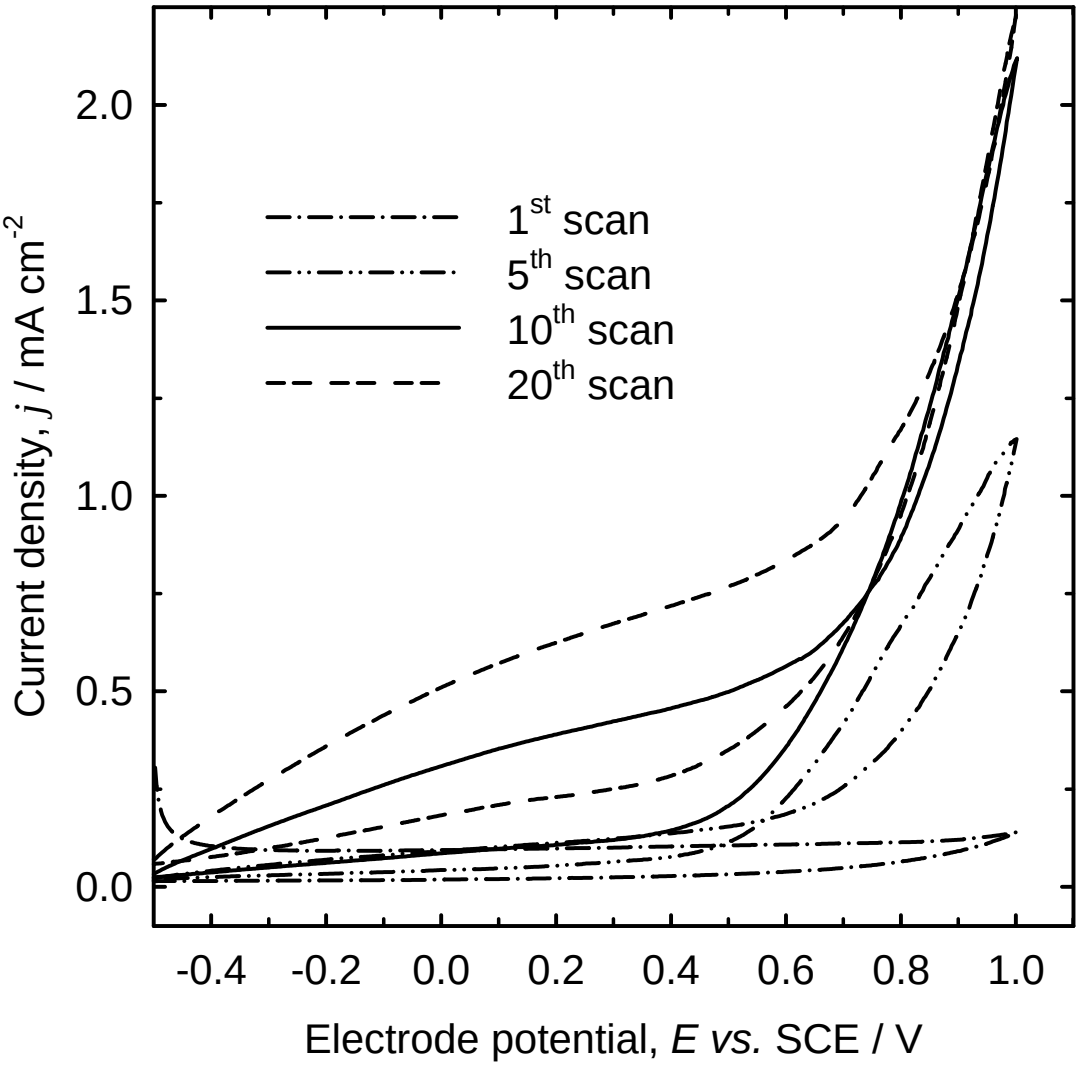
2.0
1.5
1.0
0.5
0.0
Current density, j / mA cm-2
1st scan
5th scan
10th scan
20th scan
-0.4
-0.2
0.0
0.2
0.4
0.6
0.8
1.0
Electrode potential, E vs. SCE / V

Figure 3a

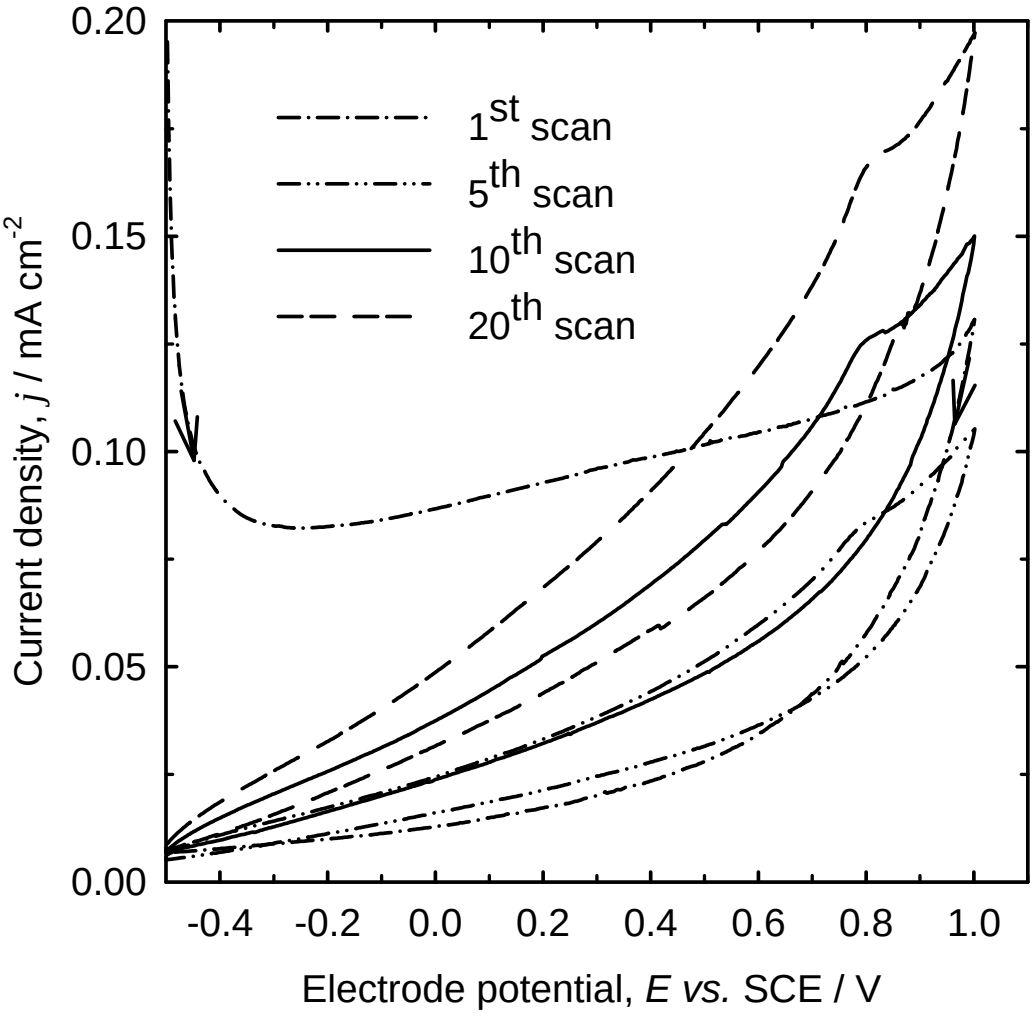
0.20
0.15
0.10
0.05
0.00
Current density, j / mA cm-2
1st scan
5th scan
10th scan
20th scan
-0.4
-0.2
0.0
0.2
0.4
0.6
0.8
1.0
Electrode potential, E vs. SCE / V

Figure 3b

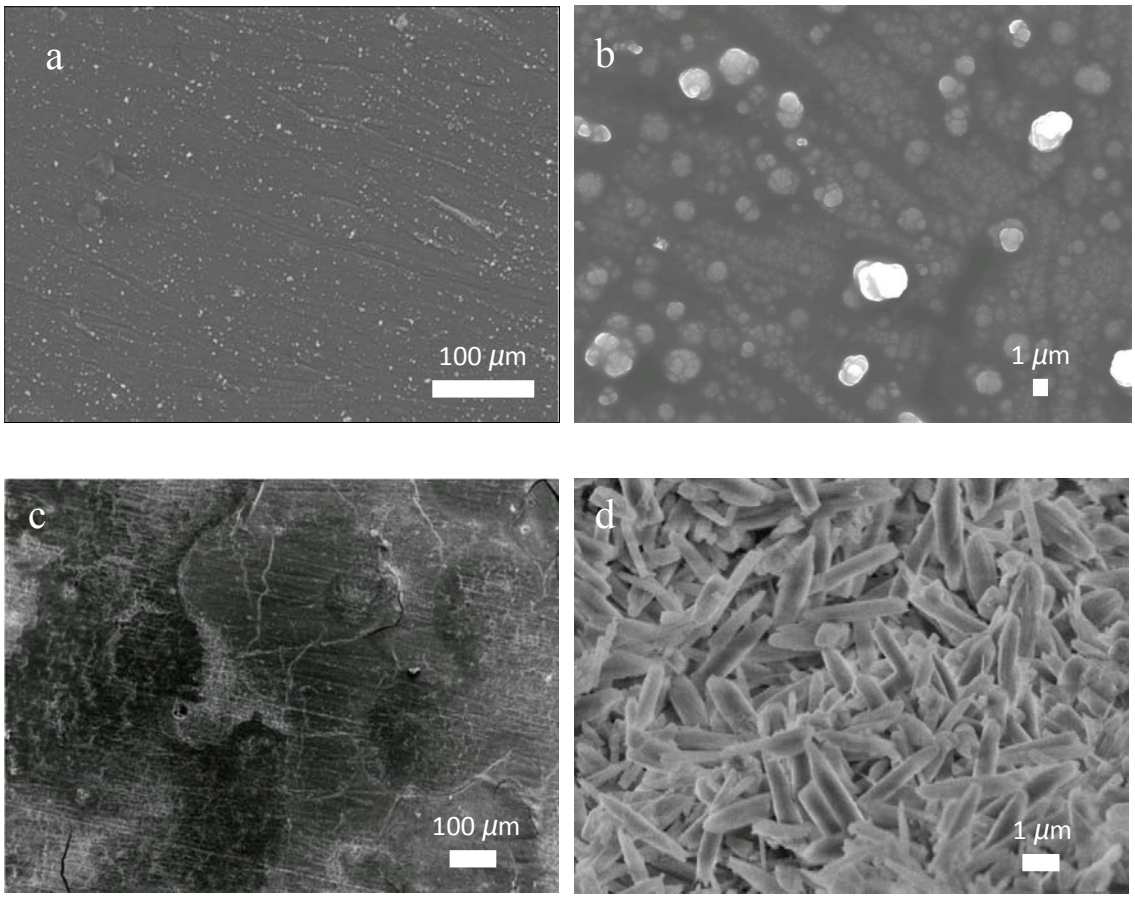

Figure 4 (a)-(d)

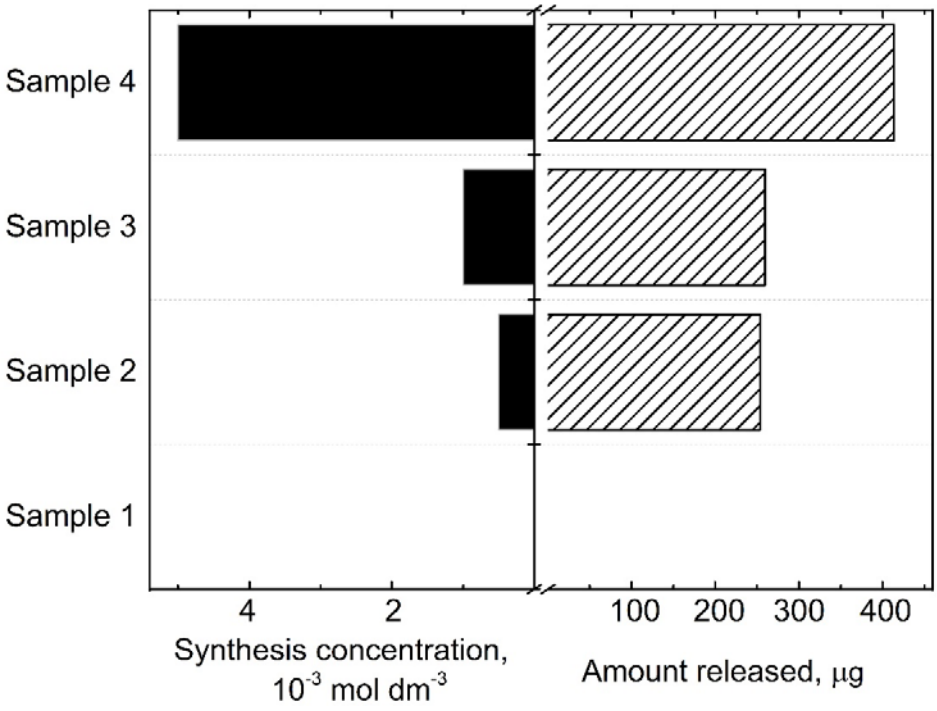
Sample 4
Sample 3
Sample 2
Sample 1
4
2
100
200
300
400
Synthesis concentration,
10-3 mol dm-3
Amount released, μg

Fig. 5

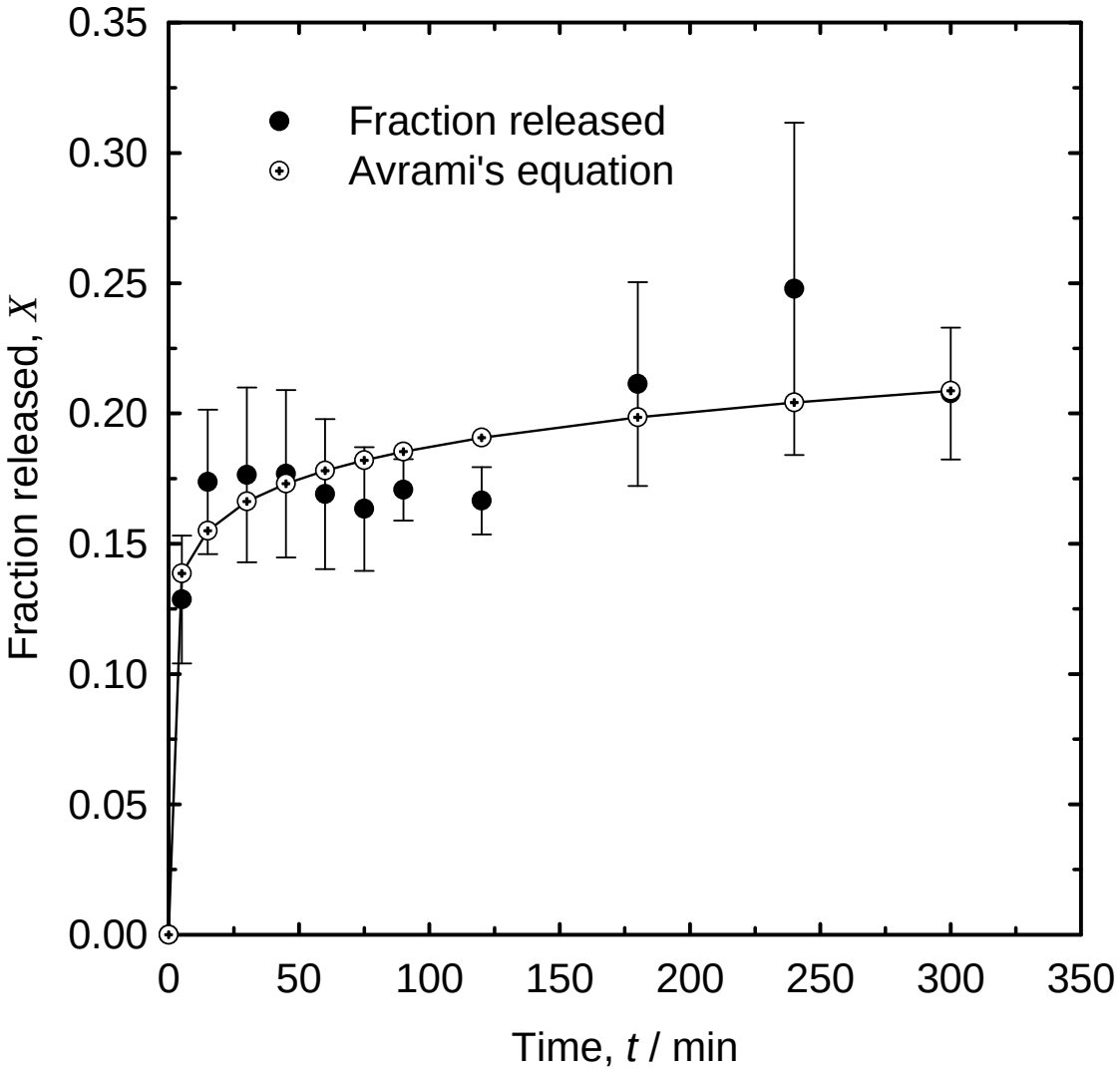
Fraction released
Avrami's equation
Fraction released, X
Time, t / min
0.00
0.05
0.10
0.15
0.20
0.25
0.30
0.35
0
50
100
150
200
250
300
350

Figure 6

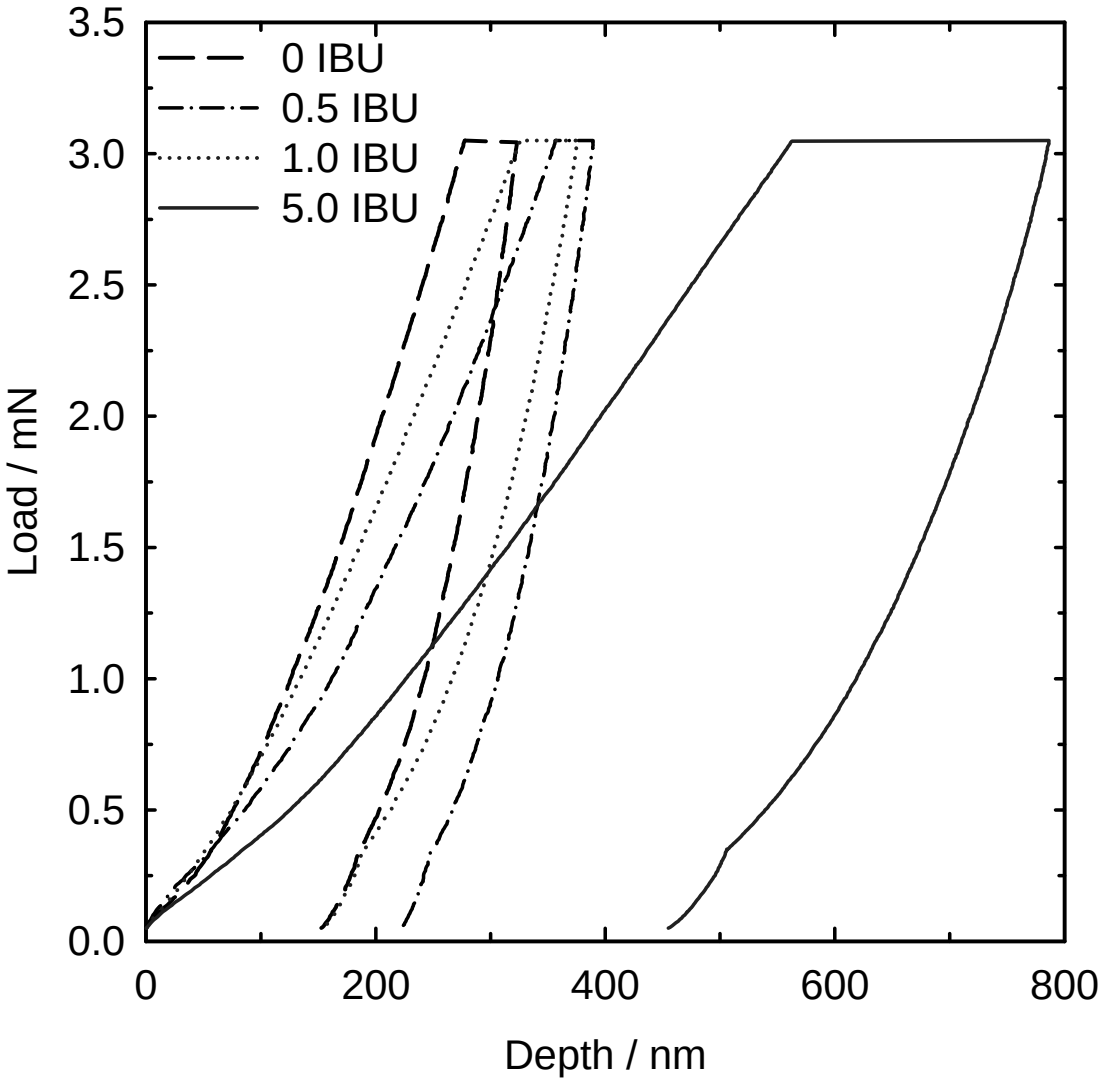
0 IBU
0.5 IBU
1.0 IBU
5.0 IBU
Load / mN
Depth / nm
0.0
0.5
1.0
1.5
2.0
2.5
3.0
3.5
0
200
400
600
800

Figure 7